OFFLINE GCSS INTERCOMPARISON STUDY OF CLOUD - RADIATION INTERACTION AND SURFACE FLUXES

Wei-Kuo Tao and Daniel Johnson
Laboratory for Atmospheres
NASA/Goddard Space Flight Center
Greenbelt, MD, 20771

(301) 614-6269
Email: tao@agnes.gsfc.nasa.gov

Abstract

Simulations of deep tropical clouds by both cloud-resolving models (CRMs) and single-column models (SCMs) in the GEWEX Cloud System Study (GCSS) Working Group 4 (WG4; Precipitating Convective Cloud Systems), Case 2 (19-27 December 1992, TOGA-COARE IFA) have produced large differences in the mean heating and moistening errors (-1 to -5 K and -2 to 2 g kg^{-1} respectively). Since the large-scale advective temperature and moisuture "forcings" are prescribed for this case, a closer examination of two of the remaining external "forcings", namely the radiational heating and air/sea heat and moisture transfer, are warranted.

This study examines the current radiation and surface flux parameterizations used in cloud models participating in the GCSS WG4, by executing the models "offline" for one time step (12 s) after given a prescribed atmospheric state, and then examining the surface and radiation fluxes from each model. The dynamic, thermodynamic, and microphysical fields are provided by the GCE-derived model output of Case 2 at 5760 min, which is during a time of active deep convection. The surface and radiation fluxes produced from the models are then divided into prescribed convective, statiform, and clear regions in order to examine the role that clouds play in the flux parameterizations.

1. INTRODUCTION

Cloud-radiation interactions have ranked as one of the most critical areas in modeling global change scenarios. Specifically, when climate-model simulations are intercompared, cloud-radiation parameterizations are found to be responsible for most of the global-mean differences in temperature sensitivity to increased greenhouse gases (Cess, 1989). This is because convective activity is the major source of water vapor in the upper free troposphere (Betts 1990; Sun and Lindzen 1993 - i.e. water vapor cloud feedback). The uncertainty in model responses is directly due to the lack of fundamental understanding of the physical processes involved in clouds. Therefore, the highest science priority identified in the Global Change Research Program (GCRP), is the role of clouds and their interaction with radiation in climate and hydrological systems. For this reason, the Global Energy and Water Cycle Experiment (GEWEX) formed the GEWEX Cloud System Study (GCSS) to address such problems. Cloud Ensemble Models (CEMs; also called Cloud Resolving Models - CRMs; or Cloud System Models - CSMs) were chosen as the primary approach for carrying out these studies (GCSS Science Plan, 1993). In addition, Single Column Models (SCMs) have been recommended for use with CEMs to examine cloud parameterizations in General Circulation Models (GCMs) and Climate Models (Randall *et al.*, 1996). Figure 1 shows a schematic diagram using the CRM and the SCM for the GCSS objectives. The CRMs use sophisticated and physically realistic parameterizations of cloud microphysical processes, and allow for their complex interactions with solar and infrared radiative transfer processes. The CRMs can reasonably well resolve the evolution, structure, and life cycles of individual clouds and cloud systems.

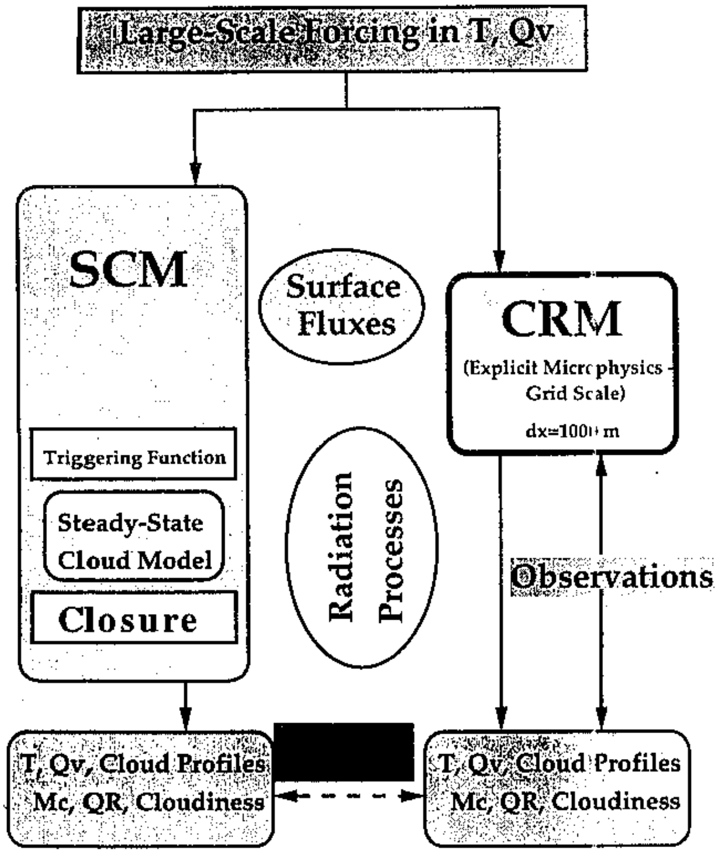

Fig. 1 Schematic diagram showing the approach of using a CEM and a SCM together for evaluating and improving the understanding of cumulus parameterization schemes. Surface fluxes and radiation could be either specified or interacted with CEM and SCM physical processes.

In the framework of the GCSS, several CRMs and SCMs were used to simulate a 7-day period in TOGA COARE (19-26 December 1992), which included several episodes of deep convection (Moncrieff *et al.*, 1997). The large-scale quantities that were required (initial conditions, upper and lower boundary conditions, large-scale advective tendencies of potential temperature and water vapor; and horizontal winds) were based on observations averaged over the COARE IFA (called a semi-prognostic approach by Soong and Ogura, 1980; and Soong and Tao, 1980). However, large differences in the mean heating and moistening errors were produced by CRMs and SCMs (-1 to -5 K and -2 to 2 g kg^{-1} respectively, see Fig. 2).

This study examines the radiation and surface flux parameterizations used in the CRMs and SCMs participating in the GCSS WG4, by executing the models "***offline***" after given a prescribed atmospheric state, and then examining the surface and radiation fluxes from each model (external - non-prescribed forcing).

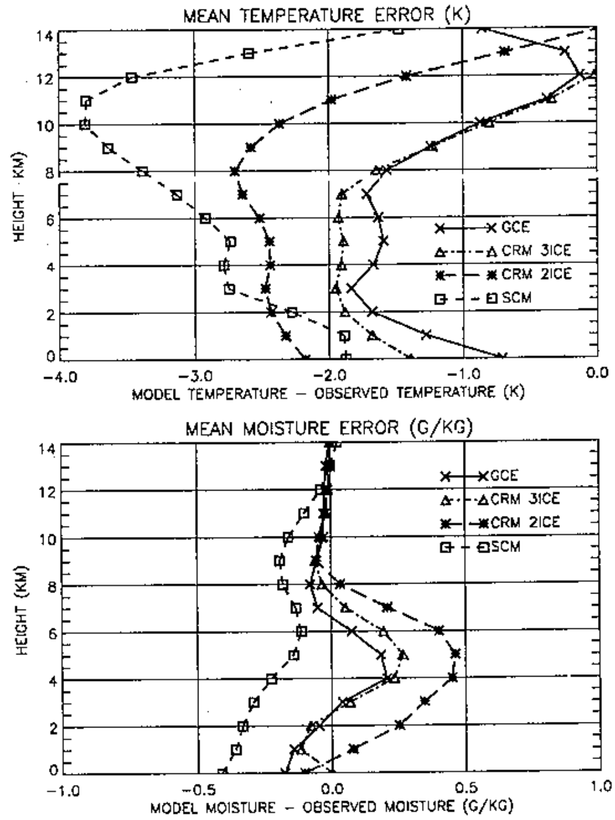

Fig. 2 Mean temperature (K), and moisture (g kg^{-1}) errors for models participating in the GCSS WG4. Models with 3-class ice physics (cloud ice, snow and graupel), produce smaller errors than models which includes only a 2-class ice scheme (cloud ice and snow). The SCMs produce larger errors due to less sophisticated physics and smaller resolution. The GCE model produced some of the smallest errors.

2. APPROACH

2.1 Data used for off-line intercomparison

The Goddard Cumulus Ensemble (GCE) model is a cloud resolving model, and its main features have been extensively published, by Tao and Simpson (1993) and Tao *et al* (1996). The model is nonhydrostatic and model variables include horizontal and vertical velocities, potential temperature, perturbation pressure, turbulent kinetic energy, and mixing ratios of all water phases (vapor, liquid, and ice). Novel characteristics of the GCE model are the explicit representation of warm rain and ice microphysical processes, and their complex interactions with solar and infrared radiative transfer processes. The dynamic, thermodynamic, and microphysical fields are provided by the GCE-derived model output of Case 2 at 5760 min, which is during a time of active deep convection. Please see web site *http://rsd.gsfc.nasa.gov/users/djohnson/gcssg4* for the GCE simulated fields used as input to the off-line model intercomparison and to examine the results.

2.2 *Convective and Stratiform partition*

In the GCE model, each grid point is designated as either a cloudy or clear area for each integration time, depending upon whether the sum of the cloud water and ice mixing ratios are larger than 0.01 g kg^{-1} at each grid point (Tao *et al.* 1987). The cloudy area can be further divided into two groups; updrafts and downdrafts. The fractional cloud area coverage as well as the cloud mass fluxes can then be diagnosed from the GCE model output. The cloud characteristics can also be divided into convective and stratiform components (Tao and Simpson 1989; Tao *et al.* 1993). Briefly, convective regions includes those with large convective velocities and/or large surface precipitation rates. Details of the GCE convective and stratiform partitioning method and its comparison with those based on radar data are described in Tao *et al* (1993). The cloud statistics in the convective component can be considered as parameterized convection in the GCM, while the stratiform component represents the prognostic cloud (GCM grid-scale resolved, see Tao, 1995).

3. RESULTS

We currently have results from five participants in the GCSS WG4 Case 2. These include the NASA/Goddard Space Flight Center GCE model (D. Johnson and W.-K. Tao), University of Utah (UU) CEM (S. Krueger and M. Zulauf), NOAA/GFDL Limited Area Nonhydrostatic model (LAN: L. Donner and C. Seman), and the United Kingdom Metor. Office (UKMO) - Large-Eddy-Model (LEM: J. Petch) and UKMO - SCM (J. Gregory). The GFDL group also submitted three different sets of results with different microphysics options (no graupel included - G-XG, graupel added to rain category - G-G>R and graupel added to snow category - G-G>S). These options do not have any impact on the off-line surface flux calculations.

3.1 Surface Fluxes

Figure 3 shows the spatial distribution of the latent heat fluxes from the four different models. Tables 1 and 2 shows the domain averaged latent and sensible heat fluxes in total, clear, convective and stratiform regions. The results indicate that the models produce large differences in the sensible and latent surface fluxes. The UKCRM produced the largest latent and sensible heat fluxes in convective regions and consequently, in the domain total. The GFDL model produces very small fluxes when compared to the other models.

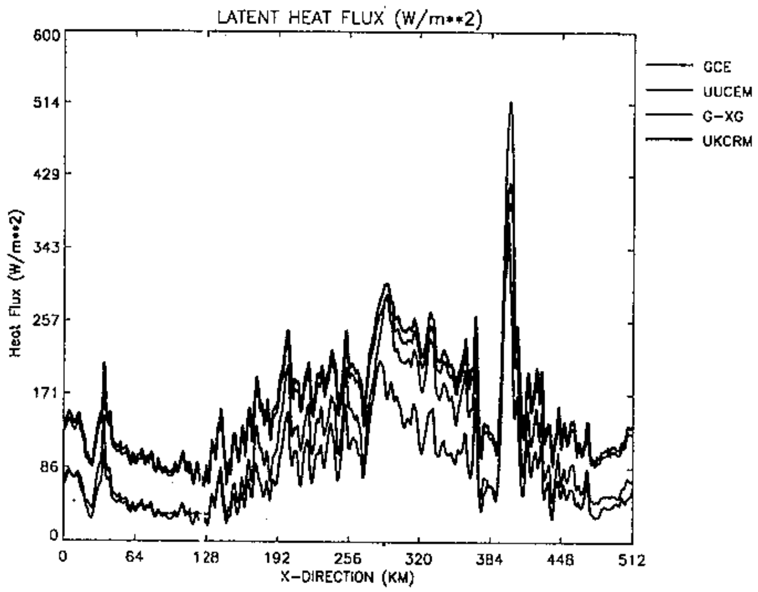

Fig. 3 Latent heat fluxes (W m-2) calculated by the four CRMs. The largest latent heat fluxes occurred at the leading edge of the convective systems with strong gust winds (generated by cold outflow).

	GCE	UUCEM	GFDL	UKCRM
Total	112.5	152.6	82.2	161.8
Clear	124.5	164.1	94.0	173.9
Convective	199.1	218.7	160.4	231.0
Stratiform	107.0	147.8	77.8	156.7

Table 1 The latent heat fluxes in domain-averaged total (512 grid points), clear, convective and stratiform regions.

	GCE	UUCEM	GFDL	UKCRM
Total	13.8	19.0	4.9	22.8
Clear	13.6	18.6	4.0	22.5
Convective	39.0	43.1	26.6	49.4
Stratiform	13.2	18.6	4.5	22.2

Table 2 The sensible heat fluxes in domain-averaged total (512 grid points), clear, convective and stratiform regions.

For the sensible and latent heat fluxes, mean differences range between 30 and 70% (4-23 W/m^2 for sensible; 10-80 W/m^2 for the latent) with consistent differences in the clear, convective, and stratiform regions. Note that the wind strengths are quite different between the three regions. The GCE model results are in good agreement with those calculated using the TOGA-COARE flux-algorithm (not shown).

3.2 Radiation Fluxes

There are two important processes that determine the cloud-radiation interactions parameterized in the SCMs and CRMs. The first one is the radiative transfer process (see Table 3). The simplest radiative radiative transfer model is that used in the MM5 (submitted by the U. of Washington for WG4). This scheme uses a broad band two-stream (upward and downward fluxes) approach for the radiative flux calculations and only requires a very small computation. The GCE model (as well as the UUCEM) uses a broad-bands radiative model. Here, the shortwave radiation models of Chou (1990, 1992) are used to compute the solar heating in the atmosphere/clouds and at the surface. The solar spectrum is divided into two regions: the ultraviolet (UV) and visible region (wavelength < 0.69 um) and the near infrared (IR) region (wavelength > 0.69 um). In the UV and visible spectral region, ozone absorption and Rayleigh and cloud scattering are included. In the near IR region, absorption due to water vapor, cloud, CO2 and O2, and scattering due to clouds are included. The UV and visible region is further grouped into four bands, and an effective ozone absorption coefficient and an effective Rayleigh scattering coefficient are given for each band. The near IR region is divided into seven water vapor absorption bands. The k-distribution method is applied to each of the seven bands for computing the absorption of solar radiation by water vapor and clouds. The four-stream discrete-ordinate scattering algorithm of Liou *et al.* (1988) is used to compute multiple scattering within a cloud layer. The simple scattering albedos for each of the seven near IR bands are taken from King *et al.* (1990). The infrared spectrum is divided into eight band and the longwave radiation model of Chou and Suarez (1994) is used to compute the cloud and atmospheric infrared cooling.The water vapor transmission function is computed using the k-distribution method, and the CO2 and O3 transmission functions are computed using look-up tables. The absorption due to cloud hydrometeors is also included while clouds are assumed to be gray and non-scattering. The multiplication approximation is used to take into account the effect of overlapping the different gas and cloud absorptions. Overall, the GFDL and UKMO both incorporate the state-of-the-art of radiative model and use multiple broad bands approaches.

The other important physical process, namely cloud optical properties, also need to be parameterized. Table 4 shows the cloud optical properties specified/parameterized in the various CRMs. Almost all of the CRMs use the cloud (liquid/ice) information to calculate the optical depth. Some CRMs also add a few additional layers above their model tops for additional radiation calculations (to eliminate large cooling or heating at the model top). Since the CRMs' resolution is less than 1 km and each grid point is either clear (0) or complete cloudiness (1). Optical depth is only calculated for each cloudy area (each grid point).

Radiation Calculations - Radiation Codes

Model	Radiative Transfer Model	Solar Albedo at sfc	IR emissivity at sfc	References
GCE 1-2	k-distribution for gaseous absorption 8 Bands for Solar; 8 Bands in IR Four-stream discrete-ordinate scattering More details	0.06	1.00	Chou, 1990, 1992, Chou and Suarez, 1994
CSU/UCLA		0.06		Harshavardhan *et al.*, 1987
CSU/RAMS	3 Bands in Solar	0.2	No Need	Harringon, 1997; Mitchell, 1997
CNRM	ECMWF	0.07	0.99	Morcrette, 1991
UW/MM5	One band	0.08	0.98	Dudhia, 1989
NCAR	NCAR CCM2	0.05	1.00	Kehl *et al.*, 1994
UU/UCLA	k-distribution for gaseous absorption 6 Bands Solar; 12 in IR Multiple scattering	0.05	1.00	Fu *et al.*, 1995; Fu and Liou, 1995
NOAA/GFDL	GFDL	0.07	1.00	Held *et al.*, 1993

Table 3 Major characteristics of the radiative transfer model used in the various CRMs. The references of these radiative transfer model are also listed.

The results indicate that the models produce large differences in the radiative fluxes, and radiative heating/cooling rates (Figs. 4 and 5). The solar heating is quite similar between all five radiative transfer schemes. The differences are mainly caused by the cloudy region. This result implies that different cloud optical properties used in the CRMs and SCMs is the main reason for the differences in shortwave heating. However, the differences in the longwave cooling is quite significant even in the clear region.

Radiation Calculations - Cloud Optical Properties

Model	Cloud water	Cloud ice	Rain	Snow	Graupel/ hail	Frequency (second)	Layers + Model Top	Cloudiness	References
GSFC/GCE-1	0.0003 cm	T, size spectra	T, size spectra	T, size spectra	Size spectra	180	7 - 0.01 mb	1, 0	Sui *et al.*, 1994; Tao *et al.*, 1996
GSFC/GCE-2	0.0003 cm	T, size spectra	T, size spectra	Size spectra	Size spectra	180	7 - 0.01 mb	1, 0	Johnson et al., 1998
CSU/UCLA	Gamma	Gamma	Size spectra	Size spectra	Size spectra	600	2	Max overlap (?)	Xu and Randall, 1995
CSU/RAMS	Gamma	Gamma	Gamma	Gamma	Gamma	100	?	1, 0	Slingo and Schrecker, 1982; Walko et al., 1994
CNRM	0.0015	0.0040	No	No	No	60 and 900	2 - 10 mb	?	Morcrette, 1991
UW/MM5	?	As Cloud water	10 Times of Cloud water	10 Times of Cloud water	No	1800	50 mb	1, 0	Dudhia, 1989
NCAR	0.0010	0.0030	Size spectra	No	Size spectra	150	40 km	1, 0	Kiehl et al., 1994
UU/UCLA	0.0010	0.0030	Size spectra	Size spectra	Size spectra	300	2 - 0.2 mb	1, 0	Fu and Liou, 1995; Fu *et al.*, 1995
NOAA/GFDL	0.0005	0.0005	0.0005	0.0005	0.0005	600	75 mb	1, 0	Held *et al.*, 1993

Table 4 The cloud optical properties (in various types of hydrometeors) assumed in the different CRMs. The frequency of calling the radiative transfer model are shown.

We also note that the differences in the radiative rates in the cloudy or stratiform regions are much more pronounced for shortwave fluxes (310-315 W m^{-2}) than for longwave (9-28 W m^{-2}) at both the surface (downward) and top-of-atmosphere (upward). Differences are also much smaller in the clear regions, but yet significant for the shortwave fluxes (14-29 W m^{-2}) and less so for the longwave (2-5 W m^{-2}).

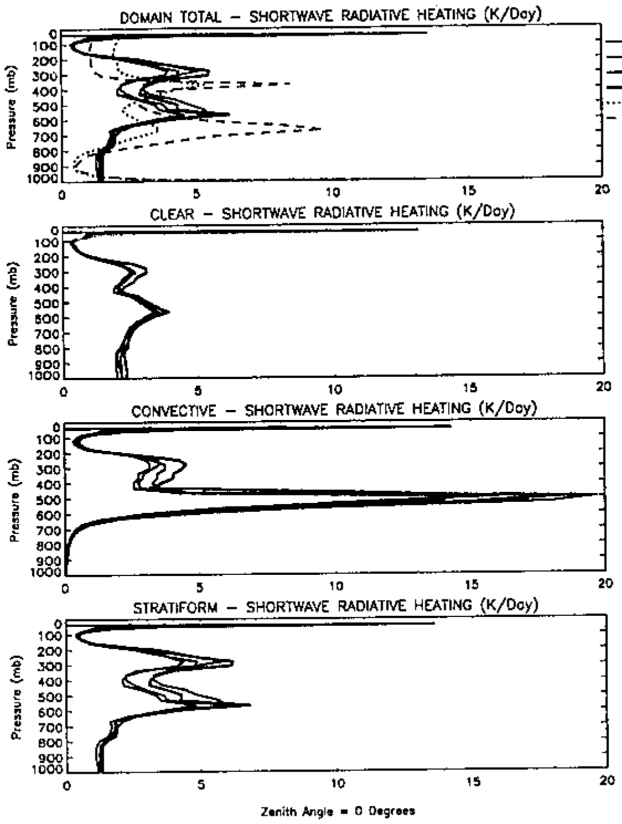

Fig. 4 The vertical distribution of the shortwave radiative cooling/heating rates performed by the off-line radiative calculations from five CRMs and a SCM. The heating/ cooling profiles in domain total, clear, convective, and straftform regions are shown in K day^{-1}.

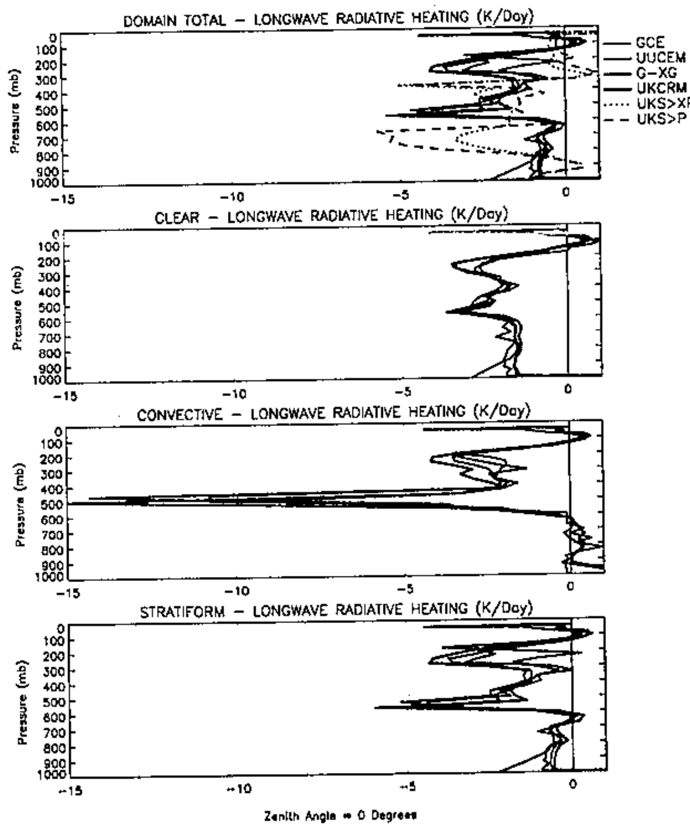

Fig. 5 Same as Fig. 4 except for the longwave cooling rate.

Acknowledgement

The author is supported by the NASA Headquarters physical climate program, the NASA TRMM, and the interdisciplinary program of EOS. Dr. M.-D. Chou provided the radiative transfer code and Dr. Y. Wang implemented the TOGA COARE flux algorithm into the GCE mode. The author is grateful to Dr. R. Kakar for his support of this research. Acknowledgment is also made to NASA/Goddard Space Flight Center for computer time used in this research.